Modeling Bimolecular Reactions and Transport in Porous Media Via Particle Tracking

Dong Ding

Hydrological Science and Engineering, Colorado School of Mines, Golden, CO, 80401, USA. (dding@mines.edu)

David A. Benson

Hydrological Science and Engineering, Colorado School of Mines, Golden, CO, 80401, USA. (dbenson@mines.edu)

Amir Paster

Environmental Fluid Mechanics Laboratories, Dept. of Civil Engineering and Geological Sciences, University of Notre Dame, Notre Dame, IN, USA

Diogo Bolster

Environmental Fluid Mechanics Laboratories, Dept. of Civil Engineering and Geological Sciences, University of Notre Dame, Notre Dame, IN, USA

Abstract

We use a particle-tracking model to simulate several one-dimensional bimolecular reactive transport experiments. In this numerical method, the reactants are represented by particles; advection and dispersion dominate the flow of particles, and molecular diffusion dictates, in large part, the reactions. The reactions are determined by the probability that reactant particles occupy the same volume over a short time interval, which is dictated by diffusion and leads to significant, mixing-limited reaction rates. The numerical model is based on the calculated probabilities of particle collisions, and as such lacks empirical parameters except for the user-defined number of particles. This number is theoretically tied to the concentration statistics and can be estimated if information about concentration autocovariance is gathered in an experiment. The simulations compare favorably to two physical experiments. In one, the product concentrations were measured at the end of a column at different times (the breakthrough curve); the other mea-

sured the distribution of reactants and products within a translucent column (snapshots). In addition, one experiment used reactants with a well-mixed thermodynamic rate coefficient 10^7 times greater than the other. The higher rate can be considered an essentially instantaneous reaction. When compared to the solution of the classical advection-dispersion-reaction equation with the well-mixed reaction coefficient, the experiments (and the particle-tracking simulations) showed on the order of 20% to 40% slower reaction attributed to poor mixing. In addition to model performance, the advantage of the Lagrangian model in this study is the lack of empirical parameters or assumptions.

Keywords: Lagrangian Particle Method, Chemical Reactions
PACS: 02.50.Ey, 02.50.Ga, 02.70.Ns, 05.10.Gg

---

1. Introduction

Reactive transport in porous media takes place in a range of environmental processes, such as water chemistry evolution [1, 2] and chemical/biochemical remediation of contaminated groundwater [3, 4, 5, 6, 7]. However, the spreading and reaction of reactive species as they migrate in the porous media is not only difficult to measure [8, 9, 10, 11, 12, 6], but simulations across a range of scales, from pore scale to field scale (e.g., [8, 13, 14, 15, 2, 16]), reveal that the overall reaction rate is subject to a scale effect [13, 17, 7, 18]. An understanding developed through experimental observations (e.g., [3, 4]) that incomplete mixing leads to reduced reaction rates or even different governing differential equations at larger scales [19, 20, 21]. Different conceptual models have been proposed to characterize reactive transport process [22, 6, 10, 23], and a variety of laboratory experiments (e.g.,[3, 4, 16]) and field-scale studies (e.g., [24, 25, 26, 27, 28]) have been conducted in order to either test the validity of existing models or to obtain effective parameters for practical problems, like groundwater remediation modeling.

One common approach to simulate Fickian transport and reaction in porous media is using the advection-dispersion-reaction equation (ADRE)

$$\partial C_i/\partial t = -\nabla \cdot (\mathbf{u}C_i - D\nabla C_i) - r_i \tag{1}$$

where $C_i(\boldsymbol{x}, t)$ is a deterministic concentration, $\mathbf{u}(\boldsymbol{x}, t)$ is the Darcy scale pore water velocity, $D(\boldsymbol{x}, t)$ is the hydrodynamic dispersion tensor most commonly modeled as linear with velocity magnitude, and $r_i(\boldsymbol{x}, t, C_1, C_2, ...)$ is

the reaction rate of species i. The reaction rate, a crucial term in ADRE, is commonly estimated from batch tests under perfect mixing conditions of the same reaction [3, 19, 18, 29, 30, 7]. When this reaction rate is used in (1) to predict miscible displacement and reaction in column- and field-scale tests, the true reaction rate is typically overestimated by significant amounts [19, 21, 31, 14]. This points to several deficiencies of the ADRE, including these (not mutually exclusive) factors: i) the deterministic concentration neglects small-scale fluctuations [3, 4, 29, 32]; ii) the reactants are assumed to be well-mixed, which is unusual under natural conditions [19, 32, 23], and iii) the dispersion term is forced to account for both the spreading and the dilution, or mixing, of the species [33, 34].

In real and synthetic tests, the spreading rate can surpass the mixing rate [14, 35, 36, 37, 38, 39]. *Cirpka and Kitanidis* [33] and *Cirpka et al.* [40, 41] point out that the bulk of actual mixing is often limited to transverse dispersion and diffusion, which is orders of magnitude lower than longitudinal dispersion.

In practical applications, to account for the over-estimated reaction in ADRE, a constant (< 1), called the effective reaction coefficient, is commonly applied to the reaction rate [4, 29, 19, 42]. Unfortunately, the coefficient value is difficult to determine and varies from case to case (and scale to scale) [19, 30]. In a series of numerical and laboratory experiments using simple bimolecular reactions ($A + B \rightarrow C$), *Kapoor et al.* [30] first showed numerically that incomplete mixing following Taylor dispersion in a single tube would have suppressed reaction rates. *Raje and Kapoor* [3] constructed a glass beads-filled column and showed that the reactant product was approximately 40% less in the column than what was predicted by (1) in one-dimension ($1D$). *Gramling et al.* [4] also ran column experiments under different velocities. All of *Gramling et al.*'s experiments were similar, with overall product production of approximately 20% less in the column than predicted by (1). Because the reaction suppression was independent of velocity, one can infer that the dispersion term was not correctly accounting for mixing. The mixing deficiency was a property of the scale and the medium, but not hydrodynamic dispersion. Another salient point that may be gleaned from these studies is the effect of dimensions on simulation. The projection of concentrations in $3D$ to fewer dimensions has the effect of averaging the perturbations that may arise from "fingers" of preferential fast flow and/or pockets of slow flow that maintain highly unmixed conditions. Using lower dimensions (which may be required for computational efficiency; or may in-

deed be the only information available from a field scale tracer test) transfers this information into smoothed average concentrations and a higher effective dispersion coefficient, but does not translate into the well-mixed reactions implied by these two effects. Similarly, *Cao and Kitanidis* [43] indicated that the solute is never fully mixed at the fringes of a plume even after large diffusion times.

These observations require alternative methods to separately account for mixing, reaction, and transport [44, 31, 18]. One approach is a Lagrangian particle tracking (PT) method. The PT method simulates chemical reactions through probabilistic rules of particle collisions, interactions, and transformations [1, 20, 45]. The general Lagrangian framework has given rise to several algorithms that represent smaller-scale physics in different ways. For example, the smoothed particle hydrodynamics method simulates any given PDE on moving particles that serve as basis functions instead of on a fixed finite difference or finite element grid. [46, 9, 31]. Because the basis particles follow velocity characteristic curves, they honor the velocity fields that can engender poor mixing. The core of the method, however, is the assumption that, at some smaller scale, the chosen PDE for reaction is the correct one.

Another Lagrangian model makes no assumption about the form of the governing equation for reaction. Instead, *Benson and Meerschaert* [20] calculate the probability that any two particles will be co-located in any time interval. This probability is given by the small-scale transport physics, meaning that any transport mechanism (e.g., Fickian, continuous time random walks, telegrapher equation) is allowed. This probability is combined with the probability that two particles, upon co-location, will react: this second probability is the well-mixed reaction rate scaled appropriately by the number of particles. Our method is an extension of the *Gillespie* [47] method, which uses a well-mixed assumption to calculate the probability of particle co-location. After calculating the total reaction probability, each particle pair is allowed to react by comparison with a randomly drawn number. Under certain test cases, the behavior of this model can transition between well-mixed and diffusion-limited reactions, and corresponds, upon upscaling, to a different transport and reaction equation [48].

Another approach proposed by *Edery et el.* [1] simulates particle motion within a continuous time random walk (CTRW) framework. The anomalous components of transport and reaction are ascribed to the non-Fickian aspects of motion that would be shared by a conservative tracer. To simulate reactions, those authors define a key parameter, called the "prescribed

effective reaction radius," which is used to determine whether a reaction between particles will happen or not. We shall denote this parameter R_E. If particles are within the R_E, they will react; otherwise, no reaction occurs [1, 32]. This radius, like the effective reaction coefficient in the ADRE, is not easy to determine, or it is arbitrary to some degree [23]. Within this radius, all particle pairs have the same probability of reaction, losing some of the physical reality that closer pairs are more likely, but not destined to react. *Edery et al.* [1] simulated the experiment profile concentrations from [4] and showed that their simulations match experiments well by using 0.5 cm for R_E, but this value does not work well to match the experiment results from [3].

Other approaches (models) have also been proposed, such as fractional ADEs [49, 21, 50, 51], time dependent reaction rate coefficients [2, 52], perturbation models [29], and multi-rate mass transfer [53, 54, 15]. These models can be calibrated to simulate the reactive transport successfully by reproducing anomalous flux-averaged breakthrough curves [5, 23]. *Edery et al.* [32] noted that both the Fickian form of their method and the time-dependent reaction method cannot match the tails of the spatial concentration profiles of experiments. To characterize the tail edges of the product plume, some assumptions have been made about the transport process, such as space and/or time-fractional-order PDEs and tempered superdiffusion and subdiffusion terms added to the R_E method [51]. *Edery et al.* [11, 32] emphasized the advantage of truncated power law (TPL) - PT, which makes particles essentially motionless for extended periods of time. On the whole, as indicated by *Tartakovsky et al.* [23], these approaches require additional effective parameters, which can only be obtained from calibration with experimental data. In this study, we test the assumption that the bulk of the experimental observations can be explained by the application of simple, physically-based rules of transport and reaction within a Lagrangian framework.

Therefore, in this study, we simulate bimolecular reactive transport using the PT method from *Benson and Meerschaert* [20] without making additional assumptions or implementing complex numerical techniques. Advection and Fickian hydrodynamic dispersion dominate the transport of particles through the glass beads, and as they move, molecular diffusion dictates their reaction. The reaction probability purely depends on the thermodynamic rate of the chemical reaction and the distribution of particles in both space and time. An advantage of this simulation method is that no extra parameters (e.g., effective reaction coefficient, reaction radius) are needed. Another novel as-

pect of the technique is the inclusion of the KD-tree algorithm (see *Bentley* [55]) that greatly increases the computational efficiency of this Lagrangian reaction methods when analyzing potential reaction pairs.

2. Summary of Column Experiments

Because of their physical and chemical simplicity (which allows an examination of the interplay of transport and reaction), we consider the experiments conducted by *Raje and Kapoor* [3] and *Gramling et al.* [4], who conducted experiments on transport of bimolecular reaction through columns. These data have been widely used to test models are widely regarded as benchmarks of reactive transport in porous media [11, 32, 52, 51]. *Raje and Kapoor* [3] used a spectrophotometer to obtain the outflow concentrations of product from the transport and reaction of 1,2-naphthoquinone-4-sulfonic acid (NQS) and aniline (AN) in a column filled with glass beads. Their results were presented as breakthrough curves (BTC) of reaction product from the end of the column. *Gramling et al.* [4] took images of colorimetric reaction between aqueous $CuSO_4$ and $EDTA^{4-}$ within a translucent chamber packed with cryloite sand to observe the concentration distribution of reaction product within the column at different locations. The setup of these experiments were similar. Peclet numbers of both experiments were high but Reynolds numbers were sufficiently low to ensure laminar flow; dispersion was estimated to dominate over diffusion in spreading of the reactant fronts. The transport and reaction domains were quasi one-dimensional and initially saturated with one species. At $t = 0$, the other reactant was introduced at the inlet with constant concentration and injection rate.

Before performing the column experiments, reaction rate constants were obtained with high degrees of confidence from well-mixed batch experiments; dispersion and diffusion coefficients were also determined with high confidence from non-reactive tracer tests. The parameters from the two experiments under different flow conditions are summarized in Table 1.

3. Methodology of Particle Transport

Bimolecular reactions can be written as $A + B \leftrightharpoons C$. Product C can either precipitate, transport in the same manner as other consituents or degenerate to A and B spontaneously at backward reaction rate k_b. For a well-mixed system, the reaction rate can be expressed as $r_A = r_B = d[A]/dt =$

Simulation	Gramling et al.			Raje and Kapoor	
Length (cm)	30	30	30	18	18
Rate Constant ($M^{-1}s^{-1}$)	2.3×10^9	2.3×10^9	2.3×10^9	4.38×10^2	4.38×10^2
Flow Rate (mL/s)	0.0445	0.267	2.5	-	-
Pore Velocity (cm/s)	0.0121	0.0832	0.670	0.096	0.070
Dispersion Coeff. (cm^2/s)	1.75×10^{-3}	1.45×10^{-2}	1.75×10^{-1}	3.17×10^{-2}	2.31×10^{-2}
Diffusion Coeff. (cm^2/s)	7.02×10^{-7}	7.02×10^{-7}	7.02×10^{-7}	4.6×10^{-6}	4.6×10^{-6}
Concentration (M)	0.02	0.02	0.02	5.0×10^{-4}	2.5×10^{-4}

Table 1: Experimental parameters.

$-k_f[A][B] + k_b[C]$, where we denote concentrations of A and B by the bracketed quantities. In some circumstances, the backward reaction rates are not accounted for in the experiments by assuming the reaction is irreversible or deducted from the forward reaction rate; in this case, the change of a reactant concentration within a given time can be quantified as $d[A]/dt = -k_f[A][B]$.

As mentioned in the introduction, our model extends the method of *Gillespie* [47], who shows that the PT Langevin equation of reaction contains a probability that is composed of two terms. One term embodies the thermodynamics of reaction given perfect mixing. The second represents the probability of two particles being co-located. Thus, the probability of reaction should be a function of distance between A and B particles and the diffusive movement at the small (pore) scale. The closer they are to each other, the higher the reaction probability will be [56]. This concept is different from the *Edery et al.* [1] model, which uses the effective radius R_E to characterize the mixing in a binary sense—the reaction proceeds if the separation of a pair of A and B particle are within a fixed radius. *Benson and Meerschaert* [20] derived the probability density for colocation as $v(s) = \int f_A(x) f_B(s+x) dx$, where $f_A(x)$ and $f_B(x)$ denote the densities of the motions of A and B particles away from their current positions, s is the initial particle separation distance. For a time step Δt, the Gaussian local diffusion has variance $2D_m\Delta t$, and the colocation density is a convolution of two of these Gaussians, which is also Gaussian but with variance $4D_m\Delta t$, where D_m is molecular diffusion. For computational efficiency, they approximated the Gaussian with a piecewise linear "tent" function with the same variance [20]:

$$v(s) = \max\left\{0, \frac{-|s|}{24D_m\Delta t} + (24D_m\Delta t)^{-1/2}\right\}. \tag{2}$$

As discussed in detail previously [35, 57, 58], and following the Fickian

BTC of the conservative components, we simulate each particle's advection-dispersion process through the domains using the Langevin equation

$$X(t + \Delta t) = X(t) + u\Delta t + Z \cdot \sqrt{2D\Delta t}, \tag{3}$$

where Z is a standard Normal random variable, $D = \alpha_L u$, α_L is dispersivity, u is average linear flow velocity. For cases here D is a constant. As others do, for speed we use a shifted and scaled uniform [0,1] random variable $\sqrt{24D\Delta t}(U(0,1) - 1/2)$ for the last term [19, 20]. Generally, molecular diffusion is a negligible component of dispersion for high Peclet number flow [3, 4, 19]. Equation (3) describes the flow of particles in the column. The selection of Δt is based on two criteria: 1) the time interval is relatively small compared with the time that solutes flow through the column, so that the reaction probability (described below) can be much less than unity to fulfill mathematical definition of a probability; 2) the simulated results of non-reactive tracer agree with the analytical solution in general. Employing this method, the transport of two species without reaction in a column was simulated (Figure 1) to compare with the analytical solution of the advection-dispersion equation and the observation of a conservative tracer transport test in [4] .

Molecular diffusion plays an important driving role at the pore-scale. Various studies (e.g., [4, 30, 15]) revealed that the distribution of reactants and reaction at the pore scale may be dominated by molecular diffusion, which for typical transport conditions proceeds relatively slowly. Moreover, in recent studies, both *Edery et al.* [32] and *Tartakovsky et al.* [23] noticed that the slow diffusion of the reacting species into and out of plume boundaries determines the reaction rate and the slow diffusion processes are a primary reason why averaged concentration models over-predict the amount of reaction. In this study, the PT model employed assumes that molecular diffusion controls the probability of reaction. *Raje and Kapoor* [3] noted that it is molecular diffusion that alters the pure advection picture by causing actual overlap or mixing of reactant masses that leads to the reaction. Additionally, *Cao and Kitanidis* [43] and *Edery et al.* [32] point out that diffusion can smooth irregularities due to velocity fluctuations at pore scales.

3.1. Initial and Boundary Conditions

As specified in the experiments, one reactant (assigned as B) initially saturates our numerical column; some amount of the other reactant (called

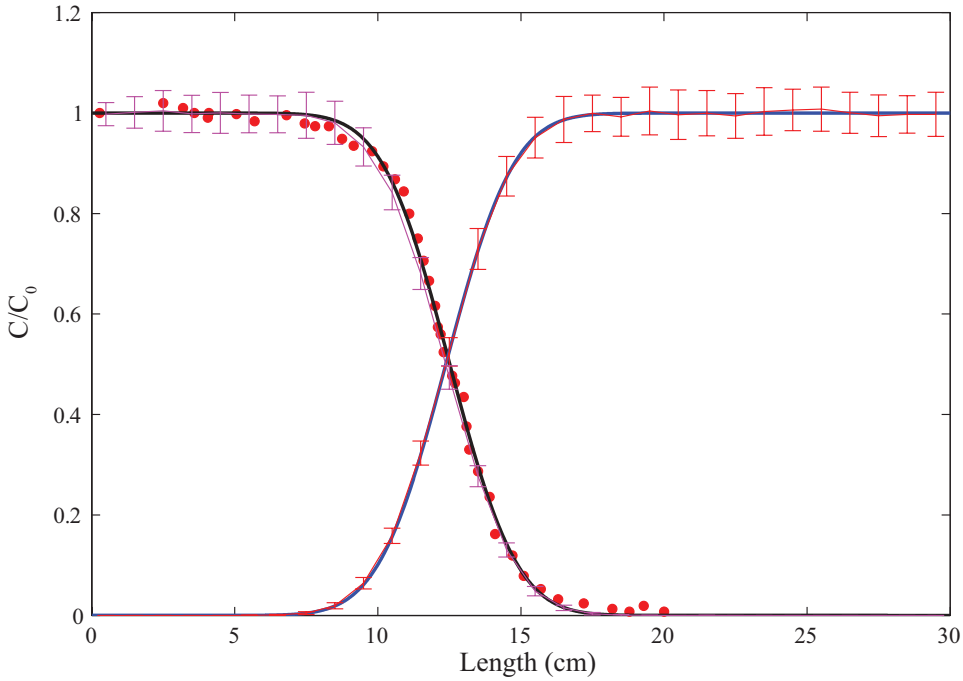

Figure 1: Verification of particle tracking concept for non-reactive transport. The red dots are breakthrough curve measurements of $CuEDTA^{2-}$ at 1023 seconds from [4]. The blue and black solid lines are analytical solutions of ADE for two species flowing through a column in which one species saturates the column initially, and the other enters at constant concentration from the upstream ($x = 0$) end. The red and magenta lines with error bars represent the simulations using PT method (equation (1)).

A) flows into the column continuously with constant flux. This implies that B particles are initially distributed within the column domain randomly and uniformly, while A particles flow into the domain at some constant rate. The initial and boundary conditions can be assumed as: $C_B(x,0) = B_0$ and $C_A(x,0) = 0$ for $x \geq 0$ (species B occupies the domain uniformly and no A species initially); $C_A(0,t) = C_0$ for $t \geq 0$ (Constant concentration of A species input at the upstream end); $C_{A,B}(L,t) = 0$ for $t \geq 0$ at the column end L (species flow out through the outlet).

At every time step, each A particle is selected sequentially to see if it will react. The KD-tree algorithm finds those B particles that are sufficiently close, and the probability of colocation is calculated, one B particle at a time. This probability is combined with the thermodynamic probability to find the total probability of reaction [20] using

$$P(react) = k_f \Delta t \Omega [B]_0 v(s)/N_0 \tag{4}$$

where the mass of each particle is given by one-dimensional column volume Ω times the initial B concentration divided by the initial number of B particles (N_0). This probability is compared with a random number between 0 and 1, which indicates whether a reaction occurs or not. If the probability of the reaction is larger than the random number, the two particles are removed from the domain and a C particle is placed randomly between the intitial A and B locations. If not, the next B particle is tested. If all potential B particles are exhausted, the next A particle is selected. This process is performed for each time step and for every A particle that is in the domain.

For *instantaneous* reaction cases where k_f is extremely large, one would have to choose prohibitively small time steps to satisfy the mathematical definition of the probability (< 1) in (4). In simulating the instantaneous reaction, the probability is assumed to be unity when two particles begin in the same location. In other words, for two particles (one A and one B) that occupy the same location ($s = 0$), they would react immediately (the probability to react is 1). To calculate the resulting *effective* k_f and Δt that can be used, calculate the known density of the tent function for initially coincident particles $v(s = 0) = \sqrt{24D\Delta t}$ and set the probability in (4) to unity ($P(react) = 1$), leaving:

$$k_f(\Delta t)^{1/2} = N_0(24D)^{1/2}/(\Omega[B]_0). \tag{5}$$

All of the parameters are known except k_f and Δt, therefore, this equation

gives a constraint on the combination of effective k_f and Δt that may be used for an instantaneous reaction.

Computation of the distances between every A and B particle is costly if a large number of particles are simulated. Classically, the computation time is a quadratic function of particle numbers times a linear function of time steps. To improve computation efficiency, only particles within a range of distance are calculated. We apply the KD-tree technique of *Bentley* [55] as implemented by *Tagliasacchi* [59], which restricts the searching objective to be within a range or a radius near the searching center. The computation time now goes like $N \log(N)$ instead of N^2, where N is the number of particles present at a given time. Thus the computational efficiency is significantly increased without reducing the accuracy.

4. Results and Discussion

In total, we simulated two sets of experiment runs by *Raje and Kapoor* [3] and six sets of experiments conducted by *Gramling et al.* [4]. Because initial locations and movements of particles are associated with random numbers in the PT method, the model results have concentration fluctuations. Physically, the fluctuations are directly linked to the incomplete mixing; as specified by *Bolster et al.* [48], when fluctuations of reactants are large relative to their mean concentration we expect the existence of isolated *'islands'* in which little or no reaction can occur, and thus the product concentration is usually lower than any prediction by a model with complete mixing. In the work by *Bolster et al.* [48], the islands arise due to initial areas that have imbalances (fluctuations) in the initial reactant distributions. These areas become islands that are enriched in one reactant as the other is reacted to depletion, and reactions can only progress by diffusion to the island edges. In these column simulations, the fluctuations are thought to arise from non-uniformity in the pore-scale flow field [3].

The results presented here are from an ensemble of one hundred simulations using the means and standard deviations for each simulation (Figures 2, 3, and 4). In addition, we reproduce the results of Figure 6a in *Gramling et al.* depicting the the cumulative mass of product formed in one experiment and simulated mass from the particle tracking method, as well as the analytical simulation of total mass in a well-mixed system (Figure 5).

Data from the two experiments were collected in different ways. *Raje and Kapoor* [3] measured the product concentrations at the outlet of the column at

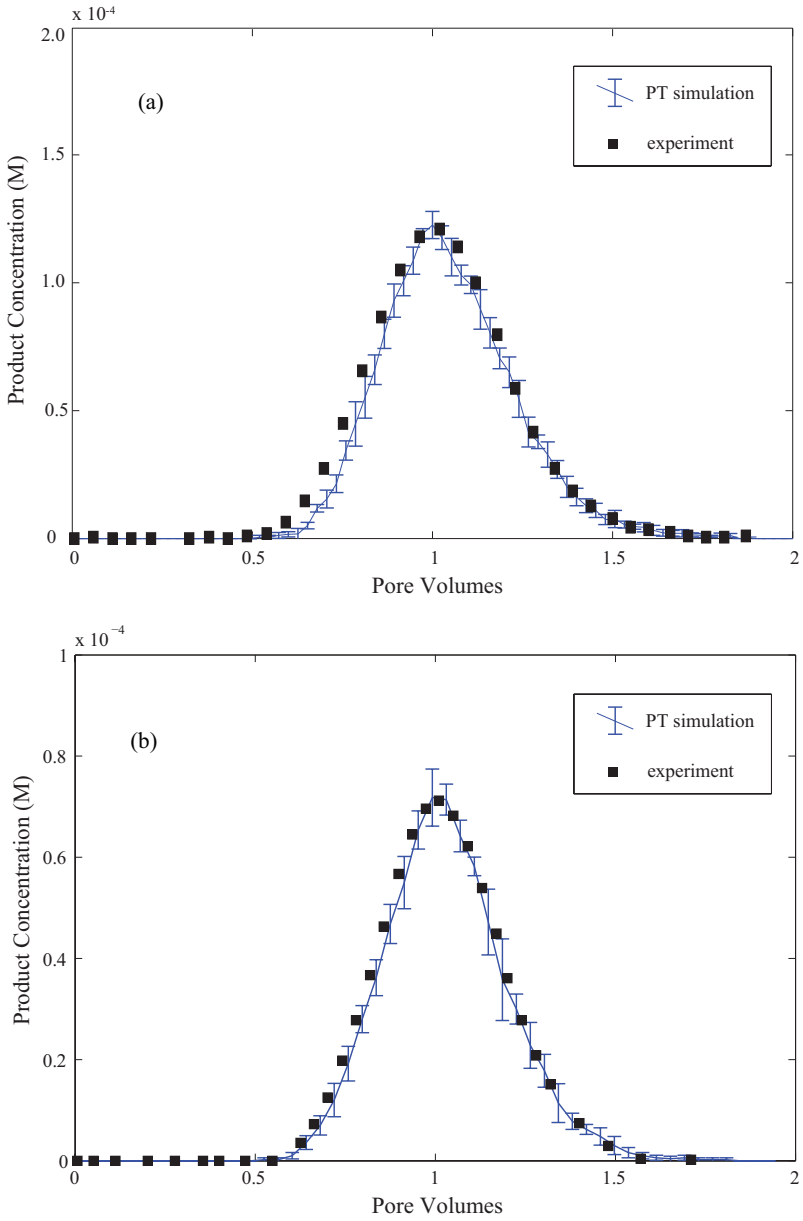

Figure 2: Simulations of experiments from [3], breakthrough curves for two experiments. Black squares are observations from the experiments, blue lines with error bars (mean values and plus/minus one standard deviation) are simulations using the PT method. a) Run 1: initial concentration of 0.5 mM, pore velocity = 0.096 cm/s. b) Run 2: initial concentration of 0.25 mM, pore velocity = 0.07 cm/s.

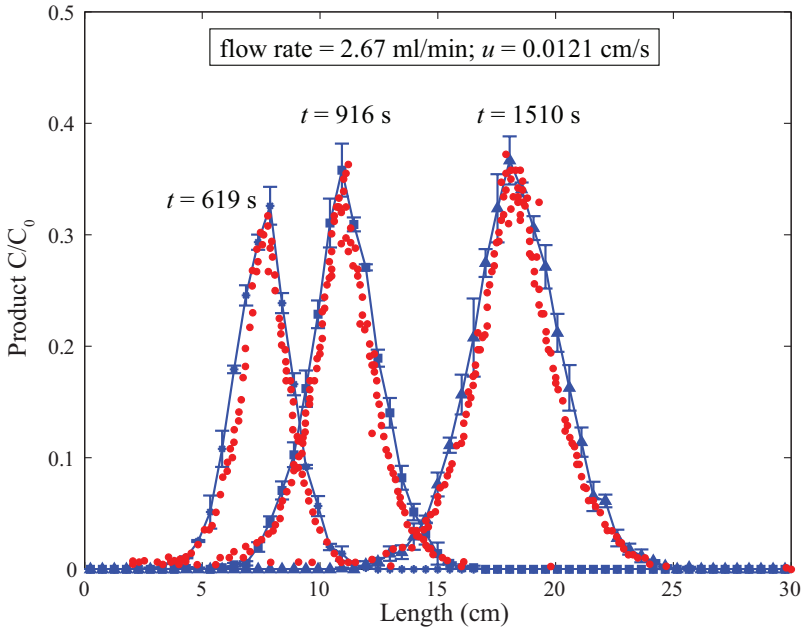

Figure 3: Simulations of the first series of experiments from [4], product concentration distributions at different times. Red dots are measurements, blue lines with error bars are simulations using the PT method. The symbols (diamond, square, and triangle) are the mean values of one hundred runs; the error bars are the standard deviations of those runs. As pointed out by *Gramling et al.*, the analytic solution of the 1D ADRE would have a peak concentration at all times of $C/C_0 = 0.5$.

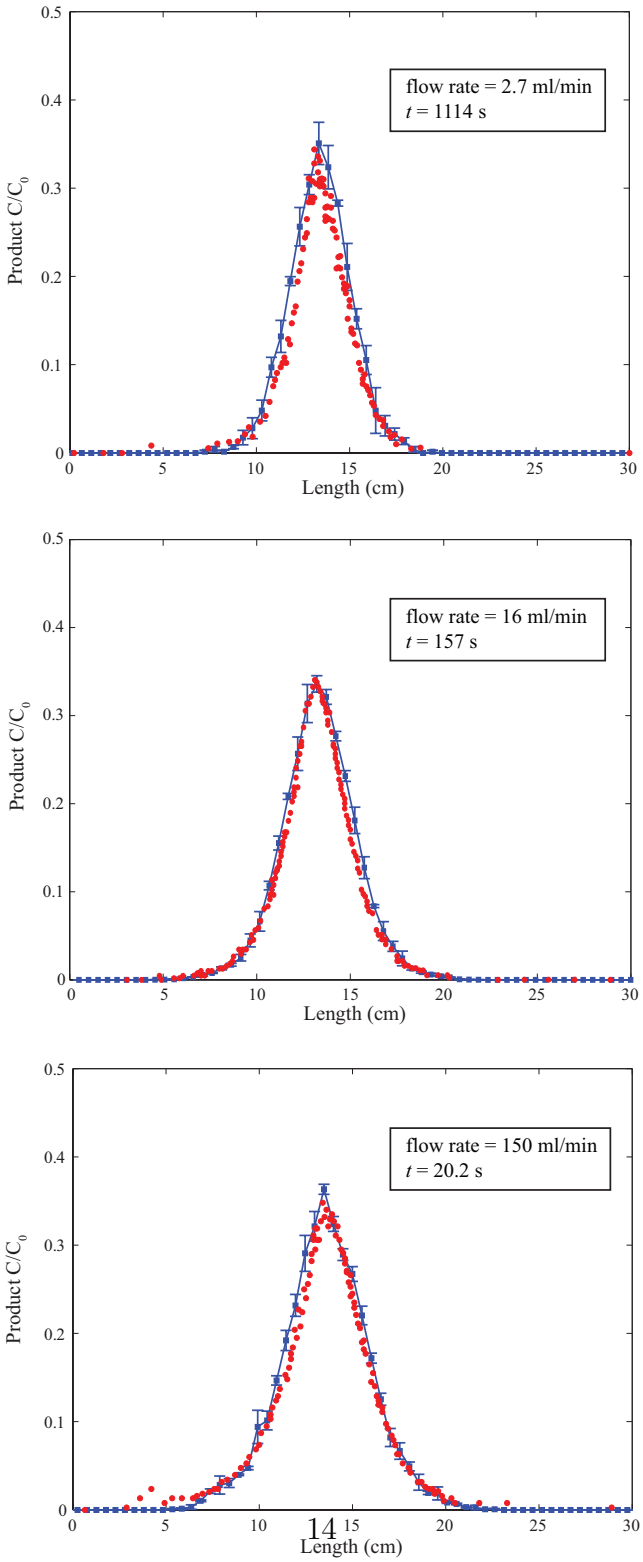

Figure 4: Simulations of the second series of experiments from [4], product concentration distribution from experiments at different flow rates. Red dots are measurements, blue lines with error bars (mean values and standard deviations of ten runs) are simulations using the PT method. a) measurements at 1114 seconds at the flow rate of 2.7 ml/min; b) measurements at 157s from experiments with flow rate of 16 ml/min; c) measurements at 20.23 seconds with a flow rate of 150 ml/min. As pointed out by *Gramling et al.*,

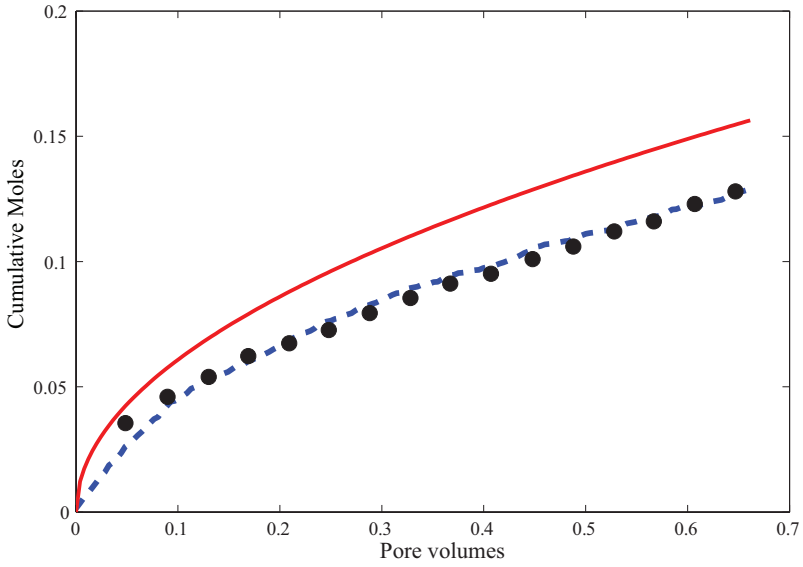

Figure 5: Total mass produced as a function of time for a flow rate of 2.7 mL/min in [4]; The solid line represents the complete mixing theoretical model results, the points are measurements, and the dashed line denotes the results from our PT model.

different times, and presented the results in the form of breakthrough curves. Those authors also simulated the experiments using a well-mixed 1D finite-difference solution of the ADRE and showed that the simulated product peak concentration was about 40% higher than the measured concentration. Their two experiments used different concentrations of reactants, $[A] = [B] = 0.25$ M and 0.5 M. We use initial numbers of particles in the PT simulations of 1000 and 2000, respectively. All other parameters were the same as those reported from experimental data, as shown in Table 1.

Gramling et al. [4] ran two series of experiments. One series had a single flow rate, and the product was tracked as it traveled across the column; the other series recorded the product concentration profiles at roughly the same place in the column under three different flow rate regimes. All the product concentrations measured in their column experiments were approximately 20% less than those predicted by an analytical well mixed solution. The first series of observations at different times had the same model parameters (e.g., flow velocity, dispersion coefficient, diffusion coefficient, time step length, etc.) except for total simulation time. For the second series of

three experiments using different flow rates, our simulations used different time step sizes following the time step rules described above. For our simulations of these two series (six datasets), the initial particle number is 600. As displayed in Figure 2, 3, and 4, most experimental data are very close to the simulated means and nearly all of them are within one standard deviation. In terms of mass balance, the simulated cumulative mass of production is also in close agreement with the measurements, as depicted in Figure 5. From this point of view, the simulations match the laboratory observations quite closely considering that no parameters are calibrated or fitted beside the number of particles used. This latter point we address shortly.

4.1. Numerical Sensitivity

To test the robustness of the model, several sensitivity analyses are run on different factors. These parameters and processes include boundary conditions, treatment of essentially instantaneous reactions, and initial particle numbers (i.e., initial conditions).

4.1.1. Boundary Conditions

One series of runs are related to the initial conditions. This is because the column experiment setup has been interpreted in different ways. For example, as Figure 5 in [3] showed, *Raje and Kapoor* [3] interpreted the initial condition of their conceptual model as the connection of columns with sharp contact. Instead of injecting some number of A particles every time step, A particles are assumed to be distributed in a hypothetical column (with the same dimensions of the experimental column) at the upstream end. The flow domain resembles two columns connected with each other, with each column initially saturated with a different reactant. We run simulations with this initial condition, the results are virtually identical to the model results shown in the Figures 2, 3, and 4.

4.1.2. Instantaneous Reactions

In reactive transport modeling, the reaction rate is generally assumed to be equal to the value reported from batch experiments [3, 19, 29]. In a Lagrangian scheme it has been hypothesized [20, 56] that the reaction probability is the product of the theromodynamic probability (including the well-mixed rate coefficient) and the probability of particle co-location. When one probability is much larger (such as in nearly instantaneous reactions), it is not the limiting factor. *Cirpka and Kitanidis* [33] made a similar conclusion

that the rate of mixing of compounds controls the reaction rate as long as the reaction process is not limited by slow kinetics.

This is not a moot point, given the disparate reaction rates in the two experiments. The reaction between $CuSO_4$ and $EDTA^{4-}$ had a high reaction rate [4] of $k_f = 2.3 \times 10^9$ $M^{-1}s^{-1}$, while the reaction rate between AN and NQS was measured with high confidence [3] to be nearly seven orders of magnitude lower ($k_f = 438$ $M^{-1}s^{-1}$). Given these rates and fairly similar experimental setups, we might expect that the concentration of product $CuEDTA^{2-}$ would be higher than that of ANNQS. On the other hand, if the results were similar, we could assume that the well-mixed reaction rate is not a limiting factor and that a range of high k_f values would give similar results. A measure of this given by the Damkohler number, which compares the timescales of reaction relative to transport processes (e.g., dispersion, diffusion). *Dentz et al.* [2] claimed that the effective rate can be virtually any fraction of the local rate depending on the Damkohler number, and the conclusion is consistent with the fact that laboratory measured kinetic rates can be orders of magnitudes larger than their field measured counterparts (e.g., [60, 61]). The diffusive Damkohler number is a dimensionless ratio of diffusion time scale ($t_D = l^2/2D_m$) over reaction time scale ($t_r = 1/A_0k_f$) [48, 34, 23], so that $D_a = t_D/t_r = A_0k_fl^2/2D_m$, where l is the size of typical concentration perturbations [L]. The length l is typically taken as the size of a pore, but may be as large as domain size [48, 19, 23]. These authors (e.g., [48, 34, 23]) define l as the typical correlation length of concentration perturbations. Given the range of correlation lengths and the reported values, the Damkohler numbers for reactions in experiments of [3] and [4] are many orders of magnitude larger than unity, which implies that time scale of diffusion in both experiments was much longer than those of the reactions. Thus the reactions can be deemed as instantaneous. Instead of using an extremely high reaction rate constant, we simulate the reaction as an instantaneous reaction.

Various studies have provided quantitative criteria to simulate the reaction as instantaneous. For instance, in derivation of transport-controlled reaction rates, *Sánchez-Vila et al.* [62] claimed that for a $D_a = 100$ or larger, the system reaches local equilibrium practically instantaneously and results using an approximation for reaction rate are almost indistinguishable from using an equilibrium reaction rate. From their point of view, to simulate the instantaneous reaction, the reaction rate constant can be chosen as long as the Damkohler number is larger than 100. *Tartakovsky et al.* [23] had

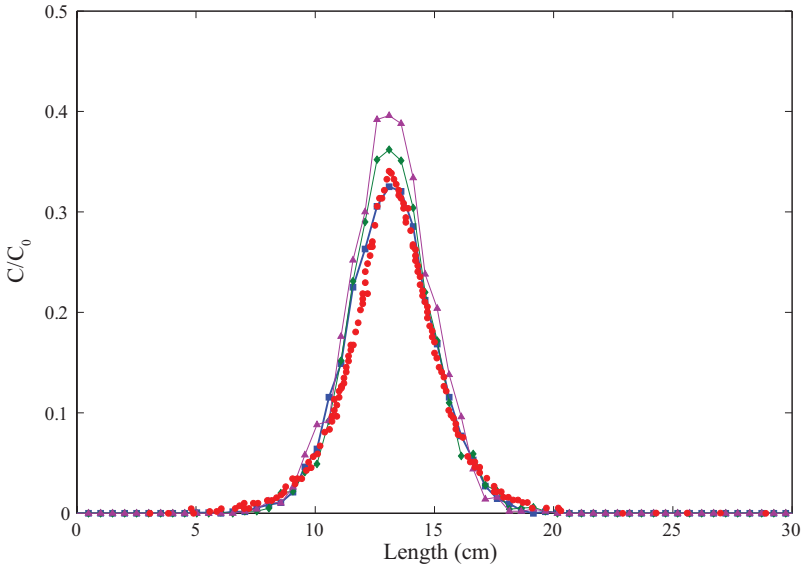

Figure 6: Simulations of instantaneous reaction with different combinations of reaction rates and time steps. The combinations of k_f and Δt lead to the maximum probability as 1, which implies that two particles would react if they occupy the same location. The combinations are 4.08 and 1 (line with squares); 12.9 and 0.1 (line with diamonds), and 40.8 and 0.01 (line with triangles).

a similar conclusion. They found that the deterministic solutions of the diffusion-reaction equation are all the same if $D_a > C_{v0}^{-1}$, where the initial coefficient of variation, $C_{v0} = \sigma_A/A_0 < 1$, where σ_A is the concentration standard deviation. In simulating the experiments of *Gramling et al.* [4], taking a conservative characteristic length value as the size of pore space, 0.13 cm, a value of reaction rate constant larger than $0.42M^{-1}s^{-1}$ satisfies the criterion of D_a (> 100). We test this by using the reaction rate over an order of magnitude larger to satisfy instantaneous reaction "criteria." Here we experimented numerically with different combinations of k_f and Δt for the reaction in experiments of *Gramling et al.* [4], as shown in Figure 6. While there is residual effect of increasing the rate coefficient, it appears that the thermodynamic part of the probability is not the determining factor in this reaction experiment. Similarly, *Edery et al.* [11] concluded that the reactions in the experiments of [4] were more controlled by fluctuations than reaction rate.

4.1.3. Particle Numbers

It may appear that, in addition to influencing the simulations, the number of particles used to represent the "plumes" of reactants is a free parameter. However, *Benson and Meerschaert* [20] showed that the number of particles is directly related to the time of onset of reactant self-segregation in simple diffusion systems. This is due to the fact that using more particles means that the reactant concentrations are smoother functions of space. Fewer particles represent more variability of concentration. *Bolster et al.* [48] took a continuum approach and showed that the variability and growth rate of initial concentration fluctuations are responsible for slowed reaction rates. In that continuum study, the authors showed that the pseudo-kinetic slowdown due to diffusion-limited mixing is directly proportional to the covariance of concentration perturbations, which they approximated with a Dirac delta function $\overline{C'_A(x,0)C'_A(y,0)} = \sigma_C^2 l\delta(x-y)$, where σ_C^2 is the early-time concentration variance and l is the correlation length representative of typical length scale associated with concentration perturbations (essentially areas of anti-correlated $[A]$ and $[B]$ denoting segregated reactants). They also showed that as long as the correlations act over relatively short spatial scales the shape of the perturbations (i.e., assuming the delta function instead of a Gaussian) is not particularly important. This enables a method to check the number of particles that should be used to represent the reactants in the columns: it has long been known for conservative solutes that the number of particles is inversely proportional to the variance of concentration [63, 64]. Therefore, the numbers of particles representing the same amount of mass should, in part, dictate the rate of reactions. As a first approximation, consider each particle individually as a delta function of concentration with covariance $\overline{C'_A(x,0)C'_A(y,0)} = (C_0^2\Omega/N_0)\delta(x-y)$ [65]. Equating the particle and continuum concentration covariance gives

$$N_0 = \frac{\sigma_{[B]}^2 l^d}{[B]_0^2 \Omega^d}. \tag{6}$$

We can roughly estimate the size and variance of concentration perturbations using the high-resolution snapshots given in [4]. We use the color images, which have integer values of red, green, and blue (RGB) saturations from 0 to 255. For a perfectly mixed experiment, any vertical transect of pixels would be the same color and have no variability in any color saturation. On the contrary, the measured vertical transects have systematic changes

in the variance of the RGB components, from the lowest value far in front of the invading fluid (Fig. 7), to the greatest in the zone of equal reactant concentrations. Using the fact that $VAR(aX) = a^2 VAR(X)$ for a constant a and assuming for this estimate that the RGB variances are additive, then the variance of concentration in the mixing zone can be estimated. The range of concentration is on the order of 0 to 0.02, while color saturations are on the order 0 to 255, or $10^{4.1}$ greater. In the area of greatest concentration contrasts, the variance of color saturation is on the order of 2000 above background noise, so that the variance of concentration is approximately on the order of $\sigma^2_{[B]} \approx 2000/10^{8.2}\mathrm{M}^2$. Furthermore, the color fluctuations have some coherent structure upon visual inspection (Fig. 7a) that can be deduced with a fast Fourier transform (Fig. 7c). Using MATLAB's FFT routine and taking the magnitude of the Fourier components for any (spatial) frequency of the color traces in vertical transect, it appears that the color traces occur in dominant frequencies with wavelengths between 25% to 100% of the column's 5.5 cm width (Fig. 8). This corresponds to fingers or "blobs" (half wavelength) of widths $l \approx 0.9$ to 2.5 cm. Using $l = 1.4$ cm (wavelength of 25 pixels, see Fig. 8) and plugging the other numbers into (6) gives an estimate of the number of particles of roughly 710, compared to the 600 we used to visually fit the reaction zones. All of the numbers used here are rough estimates, so this is by no means a quantitative validation of the approach. It is a qualitative demonstration that the theoretical number of particles is consistent with the number we used. A more concrete estimate would require more detailed measurement of concentration variance and spatial correlation.

We may test the sensitivity to this estimate by taking the simulation of the second experiment (flow rate of 16 mL/min) from [4] and holding all parameters constant, except the numbers of particles. For all three runs simulating instantaneous reaction, as shown in Figure 9, when using one order-of-magnitude lower number to represent the reactants ($N_0 = 60$), the ratio of product concentration over initial concentration is only around 0.25; when using ten times more particles ($N_0 = 6,000$), the predicted product profile (C/C_0) is approximately 0.40. As the number of particles increases to infinity, the product profile would approach 0.5, which is the maximum value in a well-mixed system (i.e., the analytic solution to the 1D ADRE (1)). From this point of view, the PT model applied in this study is capable of simulating the incomplete mixing that is characterized by high variance and/or larger concentration fluctuations by choosing a suitable number of

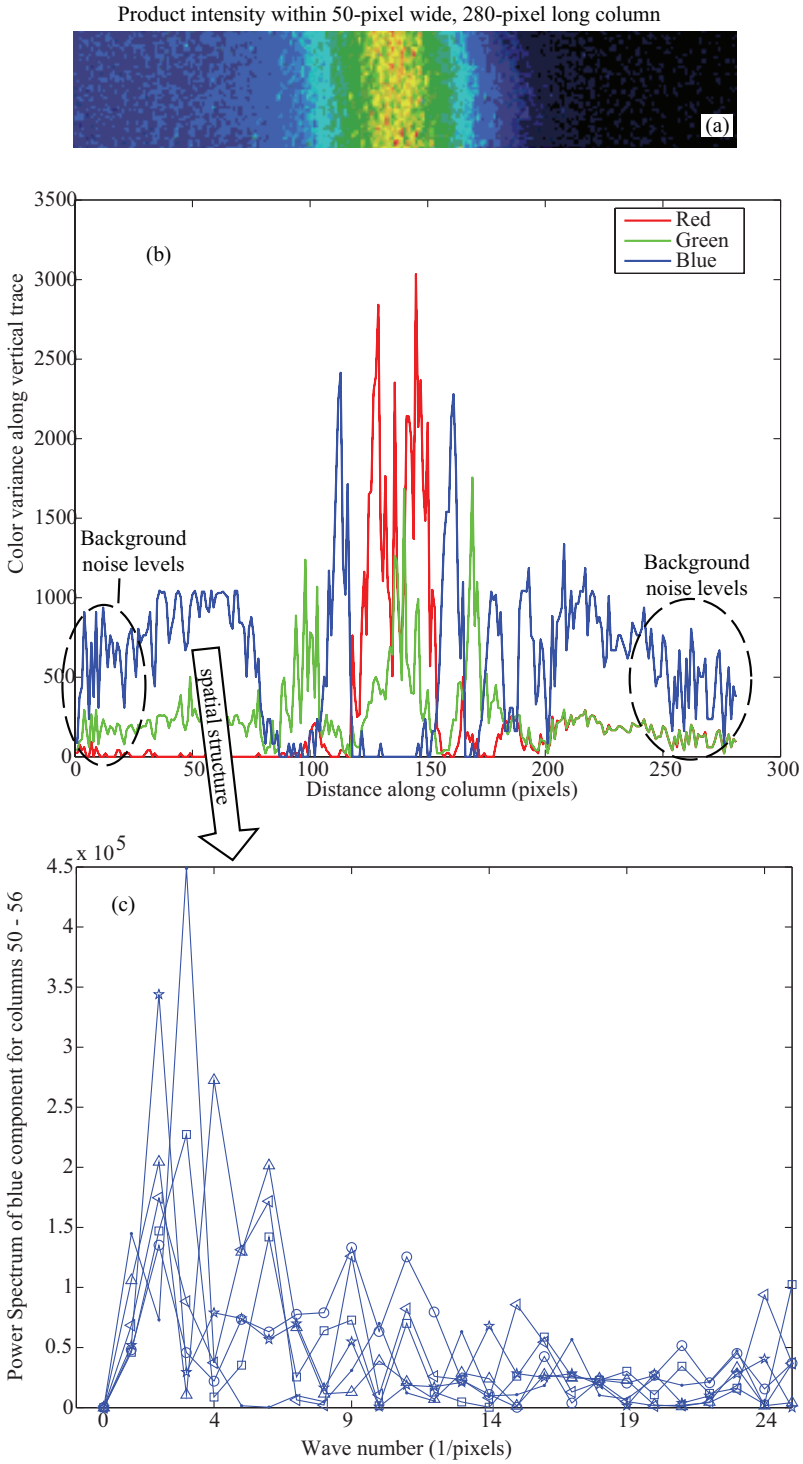

Figure 7: a) Example color map of product concentration; b) variance of red, green, and blue color components in vertical transects; c) example power spectrum of blue component in columns 50 through 56, showing dominant frequencies (wave numbers) of two to four pixels^{-1}.

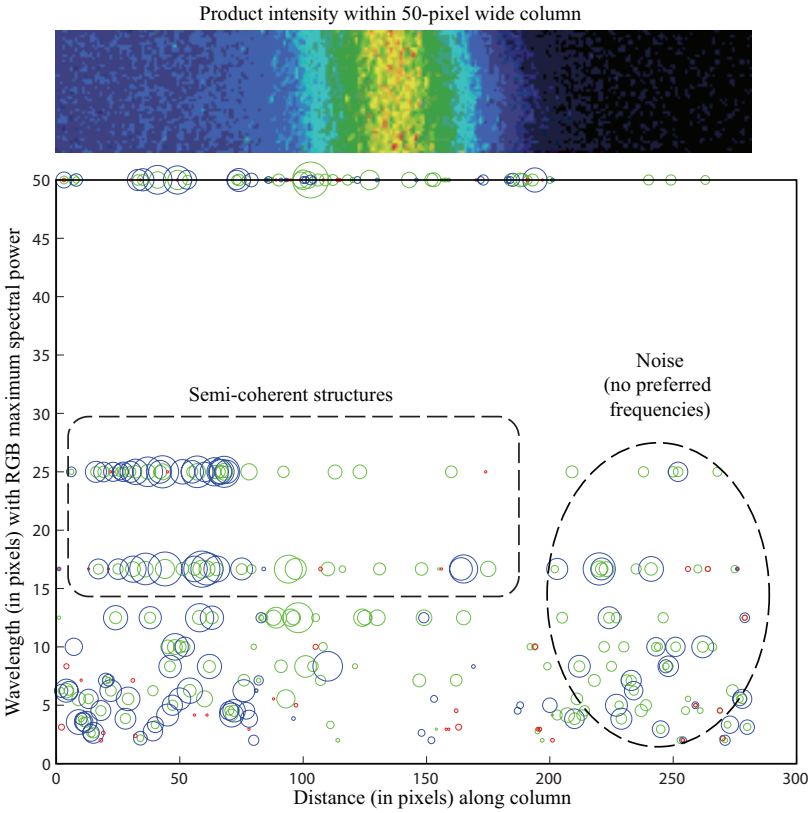

Figure 8: a) Example color map of reaction product concentrations; b) dominant wavelength from the power spectrum for each color in every vertical transect. Symbol size is proportional to spectral power. A lack of dominant wavelength, i.e., frequency, at the downstream (right) end of the column indicates uncorrelated noise.

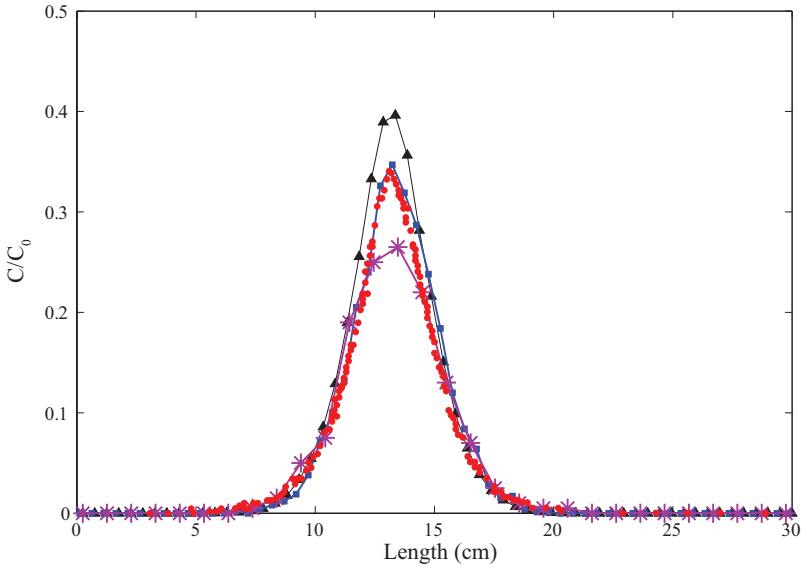

Figure 9: Effect of particle numbers, using the second experiments from [4] as base, shown as 4b. For all runs simulating instantaneous reaction, using the higher number of particles (N=6,000), the model predicted that the product concentration over initial reactant concentration was around 0.40, which overpredicts experimental observations (as red dots displays); the simulation with the lower number of particles (N=60) under predicted the measurements, the ratio was around 0.25.

particles.

4.2. Reaction Zone Tails

Besides the subdued peak product concentrations, another important finding from the two experiments is the discrepancies in the reaction zone widths. In the concentration profiles (concentration vs. length) in [4], a heavy trailing edge is seen in the product concentration not evident in the analytic solution [4, 51]. *Luo and Cirpka* [5] posit that heterogeneity leads to this extended tailing behavior in product snapshots and breakthrough curves. As reviewed by *Edery et al.* [32], models such as the ADE-PT using an effective radius approach ([11]) and the time-dependent reaction rate method ([52]), were unable to capture the forward and backward tails of the spatial concentration profiles.

To overcome this issue, *Edery et al.* [32] chose a different type of underlying solute transport. Instead of using the classical Brownian motion with the

ADE governing equation, they used a continuous time random walk (CTRW). The CTRW differs from Brownian motion in that the time required to make each motion is random and typically has a broad distribution. The heavier weights on the long-time probability tail cause some particles to delay their migrations relative to the mean, hence there is a broader spread of both reactants and products. *Zhang and Papelis* [51] extended this concept by using both random times and non-Gaussian particle migration distances to match product concentration near the tails. Both of these approaches require additional parameters that need to be gleaned from the transport experiments for a conservative tracer. It is unclear if these methods invoked to account for the tails in the reactive case were calibrated from a conservative tracer, because simulations of the non-reactive tracer test were not displayed in [32] or [51]. Furthermore, the traditional advection-dispersion equation appeared to match the conservative tracer quite well, i.e., a heavy trailing edge was not evident in the original analysis (see Figures 6 and 7 in the original [3]). In the other experiment by *Gramling et al.* [4], the conservative tails do show considerable noise that has yet to be attributed to anomalous, non-Fickian transport.

Taking a completely different view, one may theorize that any tails in the reaction product may be due simply to the addition of the reaction itself: If poor mixing or small-scale diffusion limits the reactions, then the reactants could venture farther into "enemy territory" before reacting, and the tails of the product distribution would be enlarged relative to the tails of a conservative tracer. An examination of the *Gramling et al.* experiment and our PT simulations using a logarithmic concentration axis (Figure 10) reveals greater measured product concentrations in both leading and trailing tails, as well as the ability of the PT method to model the same phenomenon.

The BTC tails in the *Raje and Kapoor* are not as straightforward (Figure 11). Because the reactions are not instantaneous, we use finite differences (FD), with $\Delta x = 0.05$ cm and $\Delta t = 0.01\Delta x/u$, to solve the ADRE (1). The measured and PT-simulated slower-flow experiment (Fig. 11a) has greater deviations from the FD solution in the tails than the faster-flow experiment (Fig. 11b). The slower-flow experiment conforms more to the instantaneous reaction assumption with high Dahmhohler numbers, so we show the (concentration normalized by $[A]_0$) finite-difference solutions on the same plot as *Gramling et al.'s* analytic solution to the ADRE (1) with instantanous reactions. The low-flow experiment deviates from the instantaneous reaction solution only near the peak, but the faster-flow experiment is roughly an

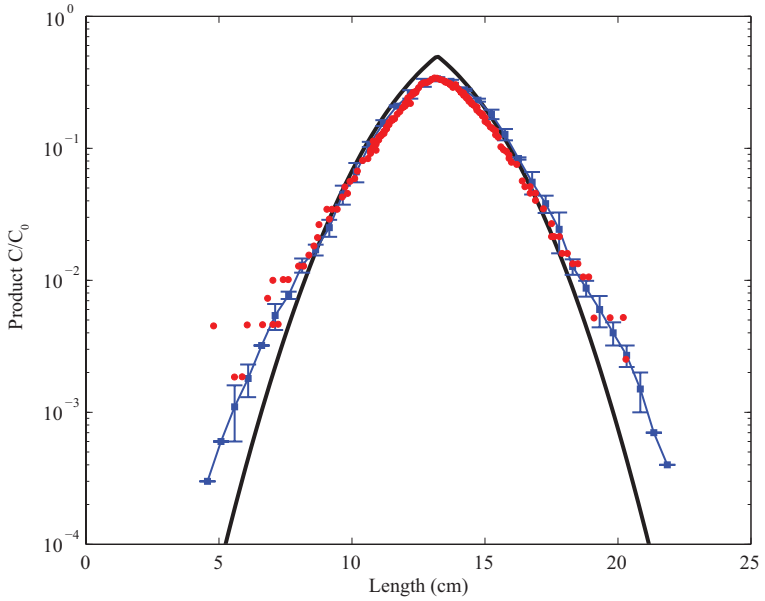

Figure 10: Semi-log plot of spatial concentration profiles from *Gramling et al.* [4]. Experimental measurements are red dots, PT simulations are blue lines through ensemble means, along with plus/minus one standard deviation, and the analytic solution of well-mixed ADRE (1) is plotted as black continuous line. These data are the same as shown in Figure 4b.

order-of-magnitude different in the tails (Fig. 11c), showing how sensitive the experiments and solutions are to small changes in flow rate at the chosen reaction rate. In all cases, the PT model applied here is capable of matching the tails in the breakthrough curves and the spatial concentration profiles without additional assumptions or parameters.

This is a significant and somewhat counter-intuitive finding. If heterogeneity was thought to merely (and uniformly) reduce reaction rates, then the measured product concentrations would be everywhere lower than the well-mixed solution. This clearly is not the case. Our PT simulations give some insight into the heavier product tails. Conceptually, some A particles may move into the displaced B particles like fingers rather than a smooth, well-mixed front. The calculation of reaction based on local diffusion allows some probability of longer particle excursions, which is consistent with the conceptualization of *Cao and Kitanidis* [43] who show that the slow rate of diffusion allows concentration gradients to be sustained at the small scale

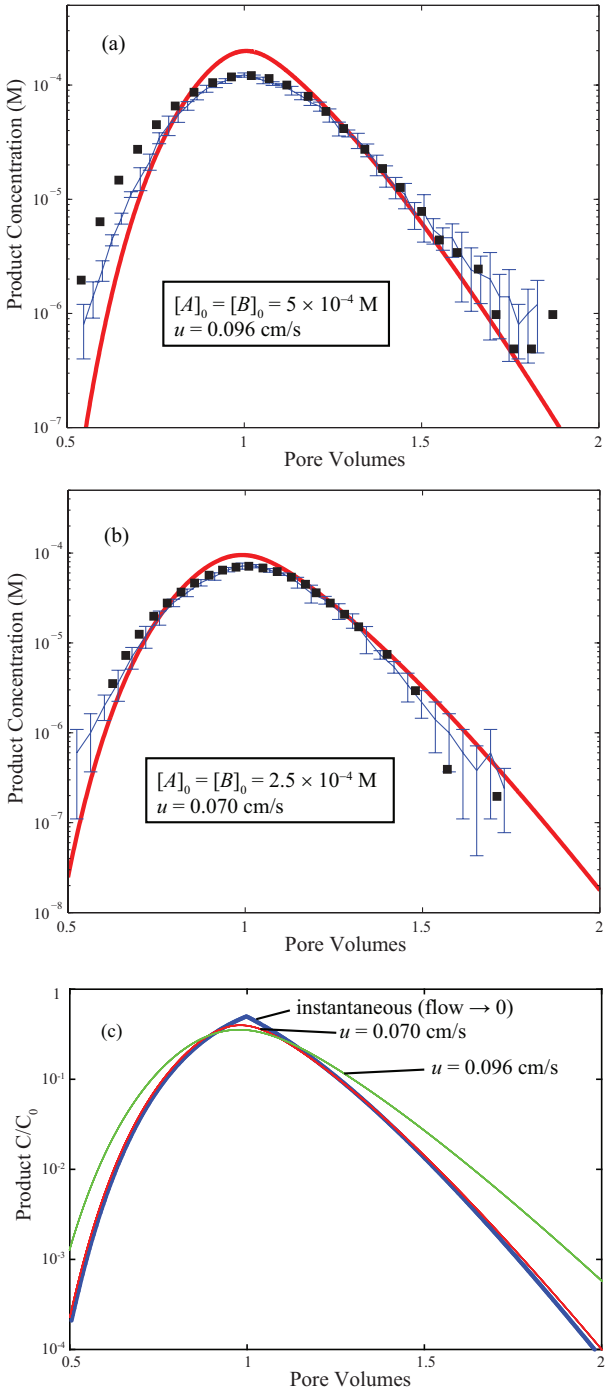

Figure 11: a and b) Semi-log plots of breakthrough curves from *Raje and Kapoor* [3]. Experimental measurements are black squares, PT simulations are blue lines through ensemble means, along with plus/minus one standard deviation, and finite-difference solutions of well-mixed ADRE (1) are plotted as red continuous lines. a) Run 1 (fast flow) experiment. b) Run 2 (slower flow) experiment. These data are the same as shown in Figure 2. c) normalized FD solutions with analytic instantaneous reaction solution.

and a reactant can cross the "interface" and interact with the other reactant only through diffusion. *Tartakovsky* [23] showed that, in a similar system (however, without the distinction between dispersion and diffusion), the rate of island or finger growth limits the rate of overall reactant mixing. This was recently shown to be identical to the random time that discrete particles require to diffuse to find a reactant partner; therefore, the particle method (with an exact calculation of co-location probability via diffusion) appears to faithfully reproduce the effects of fingering and poor mixing by segregation.

5. Conclusions and Recommendations

In this study, we implement a novel particle tracking method that calculates the probability that any two particles under general conditions of advection, dispersion, and diffusion occupy the same volume. When combined with the thermodynamic probability manifested in the well-mixed rate coefficient, the combined effects of transport and mixing-limited reaction are accurately simulated. Simulation results are tested against breakthrough curves (as function of time) reported by *Raje and Kapoor* [3] and concentration profiles through a flow domain from *Gramling et al.* [4] individually. Not only do the simulation results match the cumulative and point-wise product concentrations, but also agree with the forward and backward tails of the reaction zone. The agreements between simulations and laboratory observations suggest that this particle tracking method is able to successfully simulate the two types of experimental observations without invoking any additional transport mechanisms with their required added parameters or coefficients.

Our model is based on first principles, so that the parameters are derived from measurable quantities. The only numerical parameter with some apparent flexibility, the number of particles, represents fluctuations in concentrations, i.e., the product of concentration (spatial) variance and correlation length. This information may be gained by direct measurement of the concentration field on either small [4] or large scales [66], or by stochastic means [67, 68, 69, 19]. Using visual data of transmitted light in the experiments of [4] we derived particle numbers that matched the best-fit numbers very closely; however, the estimate is likely to have fairly large variability, the magnitude of which we do not endeavor to quantify at this point.

The particle transport and reaction algorithm presented here has yet to be extended to more complex reaction chains. This is not a theoretical problem

as reactions with multiple reactants or uneven stoichiometry are a series of two-particle interactions (see Gillespie [56]), though it may present numerical difficulties. The particle reaction algorithm also has not been coupled to detailed 3-d velocity fields for the purpose of validating, for example, *Molz and Widdowson's* [8] conjecture that poor mixing is primarily responsible for pseudo-kinetic reactions in heterogeneous flow fields at the field scale.

6. Acknowledgments

We thank ??? for thoughtful reviews. DAB was supported by NSF grants EAR–9980489, DMS–0139943, DMS–0417972, DMS–0539176, EAR–0749035, and USDOE Basic Energy Sciences grant DE-FG02-07ER15841. DB and AP were supported by NSF grant EAR-1113704. Any opinions, findings, conclusions, or recommendations do not necessary reflect the views of the NSF or DOE.

[1] Y. Edery, H. Scher, B. Berkowitz, Modeling bimolecular reactions and transport in porous media, Geophys. Res. Lett. 36 (2009) L02407.

[2] M. Dentz, P. Gouze, J. Carrera, Effective non-local reaction kinetics for transport in physically and chemically heterogeneous media, Journal of Contaminant Hydrology 120-121 (0) (2011) 222 – 236.

[3] D. Raje, V. Kapoor, Experimental study of bimolecular reaction kinetics in porous media, Environ. Sci. Technol 34 (2000) 1234–1239.

[4] C. Gramling, C. F. Harvey, L. C. Meigs, Reactive transport in porous media: A comparison of model prediction with laboratory visualization, Environ. Sci. Technol. 36 (2002) 2508–2514.

[5] J. Luo, O. A. Cirpka, How well do mean breakthrough curves predict mixing-controlled reactive transport, Water Resour. Res. 47 (2011) W02520, 12pp.

[6] Q. Kang, P. C. Lichtner, D. Zhang, An improved lattice boltzmann model for multicomponent reactive transport in porous media at the pore scale, Water Resour. Res. 43 (12) (2007) W12S14–.

[7] C. I. Steefel, D. J. DePaolo, P. C. Lichtner, Reactive transport modeling: An essential tool and a new research approach for the earth sciences, Earth and Planetary Science Letters 240 (34) (2005) 539–558.

[8] F. J. Molz, M. A. Widdowson, Internal inconsistencies in dispersion-dominated models that incorporate chemical and microbial kinetics, Water Resour. Res. 24 (4) (1988) 615–619.

[9] A. M. Tartakovsky, P. Meakin, Pore scale modeling of immiscible and miscible fluid flows using smoothed particle hydrodynamics, Advances in Water Resources 29 (10) (2006) 1464 – 1478.

[10] A. M. Tartakovsky, P. Meakin, T. D. Scheibe, B. D. Wood, A smoothed particle hydrodynamics model for reactive transport and mineral precipitation in porous and fractured porous media, Water Resour. Res. 43 (5) (2007) W05437–.

[11] Y. Edery, H. Scher, B. Berkowitz, Particle tracking model of bimolecular reactive transport in porous media, Water Resour. Res. 46 (2010) W07524.

[12] S. P. Neuman, D. M. Tartakovsky, Perspective on theories of non-fickian transport in heterogeneous media, Advances in Water Resources 32 (5) (2009) 670–680.

[13] L. Li, C. A. Peters, M. A. Celia, Upscaling geochemical reaction rates using pore-scale network modeling, Advances in Water Resources 29 (9) (2006) 1351–1370.

[14] A. Tartakovsky, G. Tartakovsky, T. Scheibe, Effects of incomplete mixing on multicomponent reactive transport, Advances in Water Resources 32 (11) (2009) 1674 – 1679.

[15] M. Willmann, J. Carrera, X. Sánchez-Vila, M. D. O. Silva, Coupling of mass transfer and reactive transport for nonlinear reactions in heterogeneous media, Water Resour. Res. 46 (2010) W07512, 15 PP.

[16] A. M. Tartakovsky, G. Redden, P. C. Lichtner, T. D. Scheibe, P. Meakin, Mixing-induced precipitation: Experimental study and multiscale numerical analysis, Water Resour. Res. 44 (6) (2008) W06S04–.

[17] S. P. Neuman, Universal scaling of hydraulic conductivities and dispersivities in geologic media, Water Resour. Res. 26 (8) (1990) 1749–1758.

[18] D. M. Tartakovsky, M. Dentz, P. C. Lichtner, Probability density functions for advective-reactive transport in porous media with uncertain reaction rates, Water Resour. Res. 45 (2009) W07414.

[19] M. Dentz, T. L. Borgne, A. Englert, B. Bijeljic, Mixing, spreading and reaction in heterogeneous media: a brief review, Journal of Contaminant Hydrology 120-121 (2011) 1–17.

[20] D. A. Benson, M. M. Meerschaert, Simulation of chemical reaction via particle tracking: Diffusion-limited versus thermodynamic rate-limited regimes, Water Resour. Res. 44 (2008) W12201.

[21] D. Bolster, D. A. Benson, T. L. Borgne, M. Dentz, Anomalous mixing and reaction induced by superdiffusive nonlocal transport, Phys. Rev. E 82 (2010) 02119.

[22] D. R. LeBlanc, S. P. Garabedian, K. M. Hess, L. W. Gelhar, R. D. Quadri, K. G. Stollenwerk, W. W. Wood, Large-scale natural gradient tracer test in sand and gravel, cape cod, massachusetts: 1. experimental design and observed tracer movement, Water Resour. Res. 27 (5) (1991) 895–910.

[23] A. M. Tartakovsky, P. de Anna, T. Le Borgne, A. Balter, D. Bolster, Effect of spatial concentration fluctuations on effective kinetics in diffusion-reaction systems, Water Resour. Res. 48 (2) (2012) W02526–.

[24] D. Ronen, M. Magaritz, H. Gvirtzman, W. Garner, Microscale chemical heterogeneity in groundwater, Journal of Hydrology 92 (12) (1987) 173–178.

[25] R. L. Smith, R. W. Harvey, D. R. LeBlanc, Importance of closely spaced vertical sampling in delineating chemical and microbiological gradients in groundwater studies, Journal of Contaminant Hydrology 7 (3) (1991) 285 – 300.

[26] J. A. Davis, D. B. Kent, J. A. Coston, K. M. Hess, J. L. Joye, Multispecies reactive tracer test in an aquifer with spatially variable chemical conditions, Water Resour. Res. 36 (2000) 119–134.

[27] K. Mayer, S. Benner, E. Frind, S. Thornton, D. Lerner, Reactive transport modeling of processes controlling the distribution and natural attenuation of phenolic compounds in a deep sandstone aquifer, Journal of Contaminant Hydrology 53 (34) (2001) 341–368.

[28] K. U. Mayer, E. O. Frind, D. W. Blowes, Multicomponent reactive transport modeling in variably saturated porous media using a generalized formulation for kinetically controlled reactions, Water Resour. Res. 38 (9) (2002) 1174–.

[29] J. Luo, M. Dentz, J. Carrera, P. K. Kitanidis, Effective reaction parameters for mixing controlled reactions in heterogeneous media, Water Resour. Res. 44 (2008) W02416, 12 pp.

[30] V. Kapoor, L. W. Gelhar, F. Miralles-Wilhelm, Bimolecular second-order reactions in spatially varying flows: Segregation induced scale-dependent transformation rates, Water Resour. Res. 33 (4) (1997) 527–536.

[31] A. M. Tartakovsky, D. M. Tartakovsky, P. Meakin, Stochastic langevin model for flow and transport in porous media, Phys. Rev. Lett. 101 (2008) 044502.

[32] Y. Edery, A. Guadagnini, H. Scher, B. Berkowitz, Reactive transport in disordered media: role of fluctuations in interpretation of laboratory experiment, Adv. Water Resour. In press, http://dx.doi.org/10.1016/j.advwatres.2011.12.008,.

[33] O. A. Cirpka, P. K. Kitanidis, An advective-dispersive stream tube approach for the transfer of conservative-tracer data to reactive transport, Water Resour. Res. 36 (5) (2000) 1209–1220.

[34] C. Knutson, A. Valocchi, C. Werth, Comparison of continuum and pore-scale models of nutrient biodegradation under transverse mixing conditions, Advances in Water Resources 30 (67) (2007) 1421 – 1431, ¡ce:title¿Biological processes in porous media: From the pore scale to the field¡/ce:title¿.

[35] P. K. Kitanidis, Particle-tracking equations for the solution of the advection-dispersion equation with variable coefficients, Water Resour. Res. 30 (11) (1994) 3225–3227.

[36] T. Le Borgne, M. Dentz, D. Bolster, J. Carrera, J. de Dreuzy, P. Davy, Non–Fickian mixing: Temporal evolution of the scalar dissipation rate in heterogeneous porous media, Adv. Water Res. 33 (12) (2010) 1468–1475.

[37] T. Le Borgne, M. Dentz, P. Davy, D. Bolster, J. Carrera, J.-R. de Dreuzy, O. Bour, Persistence of incomplete mixing: A key to anomalous transport, Phys. Rev. E 84 (1) (2011) 015301–. doi:10.1103/PhysRevE.84.015301.

[38] D. Bolster, F. J. Valds-Parada, T. LeBorgne, M. Dentz, J. Carrera, Mixing in confined stratified aquifers, Journal of Contaminant Hydrology 120–121 (0) (2011) 198–212. doi:10.1016/j.jconhyd.2010.02.003.

[39] O. A. Cirpka, P. K. Kitanidis, Characterization of mixing and dilution in heterogeneous aquifers by means of local temporal moments, Water Resour. Res. 36 (5) (2000) 1221–1236.

[40] O. A. Cirpka, E. O. Frind, R. Helmig, Numerical simulation of biodegradation controlled by transverse mixing, Journal of Contaminant Hydrology 40 (2) (1999) 159 – 182.

[41] O. A. Cirpka, F. P. J. de Barros, G. Chiogna, M. Rolle, W. Nowak, Stochastic flux-related analysis of transverse mixing in two-dimensional heterogeneous porous media, Water Resour. Res. 47 (6) (2011) W06515–.

[42] D. Ding, Transport of bacteria in aquifer sediment: experiments and modeling, Hydrogeology Journal 18 (3) (2010) 669–679.

[43] J. Cao, P. K. Kitanidis, Pore-scale dilution of conservative solutes: An example, Water Resour. Res. 34(8) (1998) 1941–1949.

[44] X. Sánchez-Vila, L. D. Donado, A. Guadagnini, J. Carrera, A solution for multicomponent reactive transport under equilibrium and kinetic reactions, Water Resour. Res. 46 (7) (2010) W07539–.

[45] T. R. Waite, Theoretical treatment of the kinetics of diffusion-limited reactions, Phys. Rev. 107 (1957) 463–470.

[46] P. A. Herrera, M. Massab, R. D. Beckie, A meshless method to simulate solute transport in heterogeneous porous media, Advances in Water Resources 32 (3) (2009) 413 – 429.

[47] D. T. Gillespie, A general method for numerically simulating the stochastic time evolution of coupled chemical reactions, Journal of Computational Physics 22 (4) (1976) 403 – 434.

[48] D. Bolster, P. de Anna, D. A. Benson, A. M. Tartakovsky, Incomplete mixing and reactions with fractional dispersion, Advances in Water Resources 37 (0) (2012) 86 – 93.

[49] D. A. Benson, S. W. Wheatcraft, M. M. Meerschaert, Application of a fractional advection-dispersion equation, Water Resour. Res. 36 (6) (2000) 1403–1412.

[50] R. Schumer, M. M. Meerschaert, B. Baeumer, Fractional advection-dispersion equations for modeling transport at the earth surface, J. Geophys. Res. 114 (2009) F00A07–.

[51] Y. Zhang, C. Papelis, Particle-tracking simulation of fractional diffusion-reaction processes, Phys. Rev. E 84 (2011) 066704.

[52] X. Sánchez-Vila, D. Fernàndez-Garcia, A. Guadagnini, Interpretation of column experiments of transport of solutes undergoing an irreversible bimolecular reaction using a continuum approximation, Water Resour. Res. 46 (2010) W12510.

[53] R. Haggerty, S. M. Gorelick, Multiple-rate mass transfer for modeling diffusion and surface reactions in media with pore-scale heterogeneity, Water Resour. Res. 31 (10) (1995) 2383–2400.

[54] L. D. Donado, X. Sánchez-Vila, M. Dentz, J. Carrera, D. Bolster, Multicomponent reactive transport in multicontinuum media, Water Resour. Res. 45 (11) (2009) W11402–.
URL http://dx.doi.org/10.1029/2008WR006823

[55] J. L. Bentley, Multidimensional binary search trees used for associative searching, Communications of the ACM 18 (1975) 509–517.

[56] D. T. Gillespie, Exact stochastic simulation of coupled chemical reactions, J. Phys. Chem. 81 (25) (1977) 2340–2361.

[57] E. M. LaBolle, G. E. Fogg, A. F. B. Tompson, Random-walk simulation of transport in heterogeneous porous media: Local mass-conservation problem and implementation methods, Water Resour. Res. 32 (3) (1996) 583–593.

[58] E. M. LaBolle, J. Quastel, G. E. Fogg, Diffusion theory for transport in porous media: Transition-probability densities of diffusion processes corresponding to advection-dispersion equations, Water Resour. Res. 34 (7) (1998) 1685–1693.

[59] A. Tagliasacchi, Matlab kd-tree library (9 2010).
URL https://sites.google.com/site/andreatagliasacchi/software/matlabkd-treeli

[60] A. F. White, S. L. Brantley, The effect of time on the weathering of silicate minerals: why do weathering rates differ in the laboratory and field?, Chemical Geology 202 (34) (2003) 479–506.

[61] L. Li, C. I. Steefel, L. Yang, Scale dependence of mineral dissolution rates within single pores and fractures, Geochimica et Cosmochimica Acta 72 (2008) 360–377.

[62] X. Sánchez-Vila, M. Dentz, L. D. Donado, Transport-controlled reaction rates under local non-equilibrium conditions, Geophys. Res. Lett. 34 (10) (2007) L10404–.

[63] E. M. LaBolle, J. Quastel, G. E. Fogg, J. Gravner, Diffusion processes in composite porous media and their numerical integration by random walks: Generalized stochastic differential equations with discontinuous coefficients, Water Resour. Res. 36 (3) (2000) 651–662.

[64] P. Chakraborty, M. M. Meerschaert, C. Y. Lim, Parameter estimation for fractional transport: A particle-tracking approach, Water Resour. Res. 45 (10) (2009) W10415–.

[65] A. Paster, D. Bolster, D. A. Benson, Particle tracking and the diffusion-reaction equation, Water Resour. Res. – (submitted) –.

[66] L. W. Gelhar, C. Welty, K. R. Rehfeldt, A critical review of data on field-scale dispersion in aquifers, Water Resour. Res. 28 (7) (1992) 1955–1974.

[67] A. Fiori, G. Dagan, Concentration fluctuations in transport by groundwater: Comparison between theory and field experiments, Water Resour. Res. 35 (1) (1999) 105–112.

[68] A. Fiori, S. Berglund, V. Cvetkovic, G. Dagan, A first-order analysis of solute flux statistics in aquifers: The combined effect of pore-scale dispersion, sampling, and linear sorption kinetics, Water Resour. Res. 38 (8) (2002) 1137–.

[69] A. Fiori, F. Boso, F. P. J. de Barros, S. De Bartolo, A. Frampton, G. Severino, S. Suweis, G. Dagan, An indirect assessment on the impact of connectivity of conductivity classes upon longitudinal asymptotic macrodispersivity, Water Resour. Res. 46 (8) (2010) W08601–.